





Cite this: *RSC Adv.*, 2024, 14, 1513

Novel phenylthiazoles with a *tert*-butyl moiety: promising antimicrobial activity against multidrug-resistant pathogens with enhanced ADME properties†

Mohamed Hagra, ^a Abdelrahman A. Abuelkhir,^a Nader S. Abutaleb,^{bc} Ahmed M. Helal,^a Iten M. Fawzy, ^d Maghawry Hegazy, ^e Mohamed N. Seleem^{bf} and Abdelrahman S. Mayhoub^{*ag}

The structure–activity relationship of a new *tert*-butylphenylthiazole series, with a pyrimidine linker, was investigated. We wished to expand knowledge of this novel class of antibiotics by generating 21 new derivatives bearing ≥ 2 heteroatoms in their side chains. Their activity was examined against isolates of methicillin-resistant *Staphylococcus aureus* (MRSA), *Clostridium difficile*, *Escherichia coli*, *Neisseria gonorrhoeae*, and *Candida albicans*. Two compounds with 1,2-diaminocyclohexane as a nitrogenous side chain showed promising activity against the highly infectious MRSA USA300 strain, with a minimum inhibitory concentration (MIC) of $4 \mu\text{g mL}^{-1}$. One of these two compounds demonstrated potent activity against *C. difficile*, with a MIC of $4 \mu\text{g mL}^{-1}$. Moderate activities against a *C. difficile* strain with a MIC of $8 \mu\text{g mL}^{-1}$ were noted. Some new compounds possessed antifungal activity against a wild fluconazole-resistant *C. albicans* strain, with MIC values of 4 – $16 \mu\text{g mL}^{-1}$. ADME and metabolism-simulation studies were performed for the most promising compound and compared with lead compounds. Our results revealed that one compound possessed greater penetration of bacterial membranes and metabolic resistance, which aided a longer duration of action against MRSA.

Received 8th November 2023
Accepted 12th December 2023

DOI: 10.1039/d3ra07619a

rsc.li/rsc-advances

1. Introduction

Antimicrobial resistance (AMR) is among the most relevant health problems of this century.^{1,2} Methicillin-resistant *Staphylococcus aureus* (MRSA) is one of the main reasons for persistent infections in humans.³ MRSA causes severe morbidity and mortality worldwide so, in 2017 the World Health Organization

considered it to be a high-priority multidrug-resistant pathogen.⁴ MRSA is responsible for serious infections resistant to most antibiotics on the market, such as skin and soft-tissue infections, bacteremia, infective endocarditis, osteomyelitis, and pneumonia. Moreover, MRSA is often responsible for infections due to indwelling catheters, prosthetic devices, and implants.^{5–7} A significant gene (*mecA*) confers to MRSA the ability to grow undisturbed in the presence of penicillin-like antibiotics. *mecA* is found in all MRSA strains and encodes penicillin binding protein 2a (PBP2a).⁸ *Clostridium difficile* has been recognized worldwide as the leading cause of nosocomial diarrhea, which is associated with substantial morbidity and mortality.^{9,10} Recent reports have suggested an increase in the incidence and severity of *C. difficile* infection.¹¹ Based on statistical analyses from the US Centers of Disease Control and Prevention, each year, more than 250 000 people need hospital care and at least 14 000 people die from *C. difficile* infection in the USA.¹²

AMR has reached alarming levels globally.^{13,14} Each year, ~750 000 deaths due to AMR are reported, and the toll is likely to grow to 10 million by 2050.¹³ Treatments for bacterial infections, including β -lactam antibiotics,¹⁵ macrolides,¹⁶ fluoroquinolones,^{16–19} glycopeptides (chiefly vancomycin)²⁰ and oxazolidinones (primarily linezolid), are increasingly becoming inadequate.²¹ Therefore, there is an urgent need to synthesize

^aDepartment of Pharmaceutical Organic Chemistry, College of Pharmacy (Boys), Al-Azhar University, Cairo 11884, Egypt. E-mail: m.hagrs@azhar.edu.eg; amayhoub@azhar.edu.eg

^bDepartment of Biomedical Sciences and Pathobiology, Virginia-Maryland College of Veterinary Medicine, Virginia Polytechnic Institute and State University, Blacksburg, Virginia 24061, USA

^cDepartment of Microbiology and Immunology, Faculty of Pharmacy, Zagazig University, Zagazig 44519, Egypt

^dDepartment of Pharmaceutical Chemistry, Faculty of Pharmacy, Future University in Egypt, 11835, Cairo, Egypt

^eBiochemistry and Molecular Biology Department, Faculty of Pharmacy (Boys), Al-Azhar University, Cairo 11884, Egypt

^fCenter for One Health Research, Virginia Polytechnic Institute and State University, Blacksburg, Virginia 24061, USA

^gUniversity of Science and Technology, Nanoscience Program, Zewail City of Science and Technology, October Gardens, 6th of October, Giza 12578, Egypt

† Electronic supplementary information (ESI) available. See DOI: <https://doi.org/10.1039/d3ra07619a>



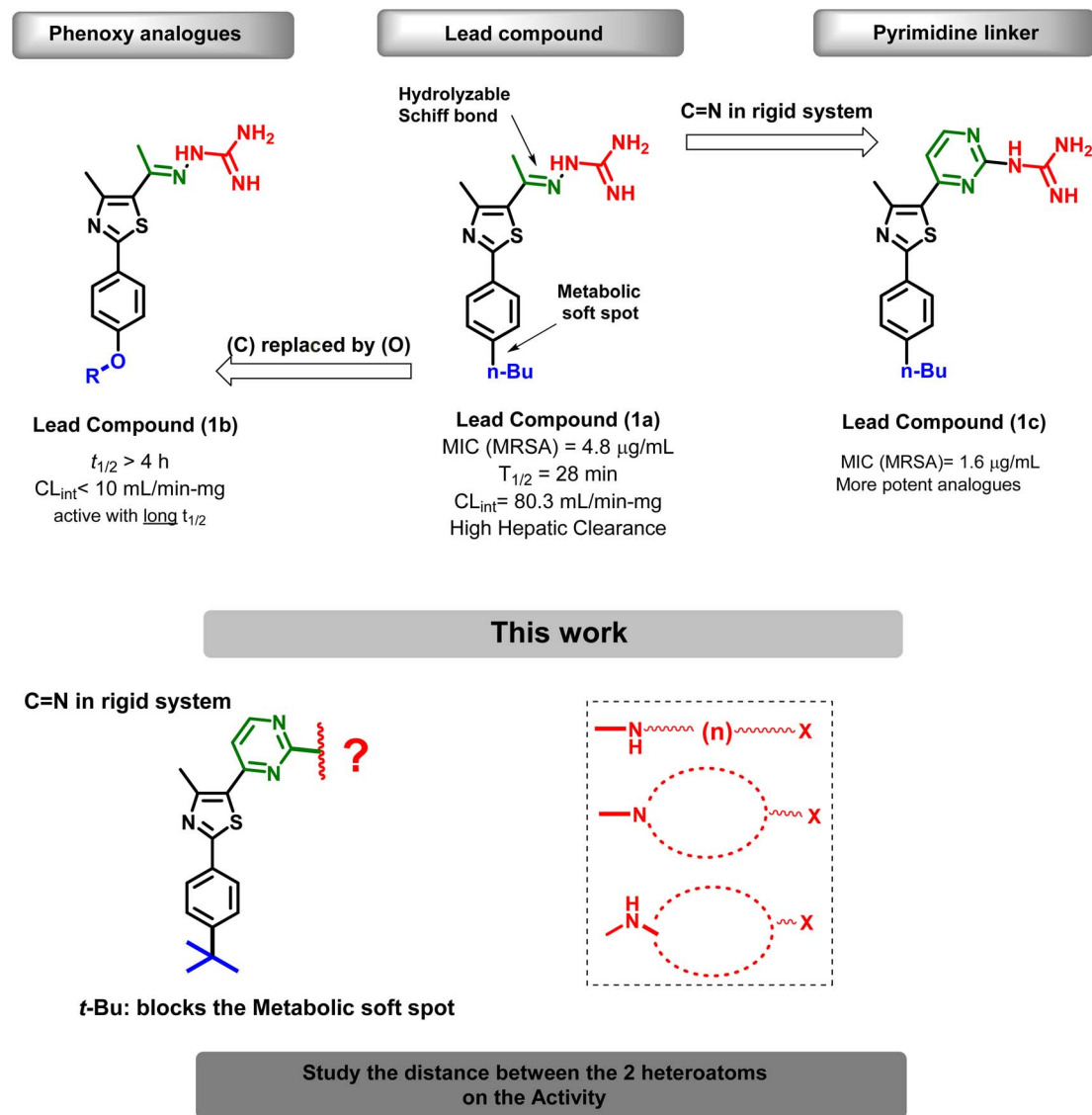


Fig. 1 Developmental progress of phenylthiazole antibiotics and a new approach to improve metabolic stability and activity.

novel antibiotics to overcome the main mechanisms for bacterial resistance.²²

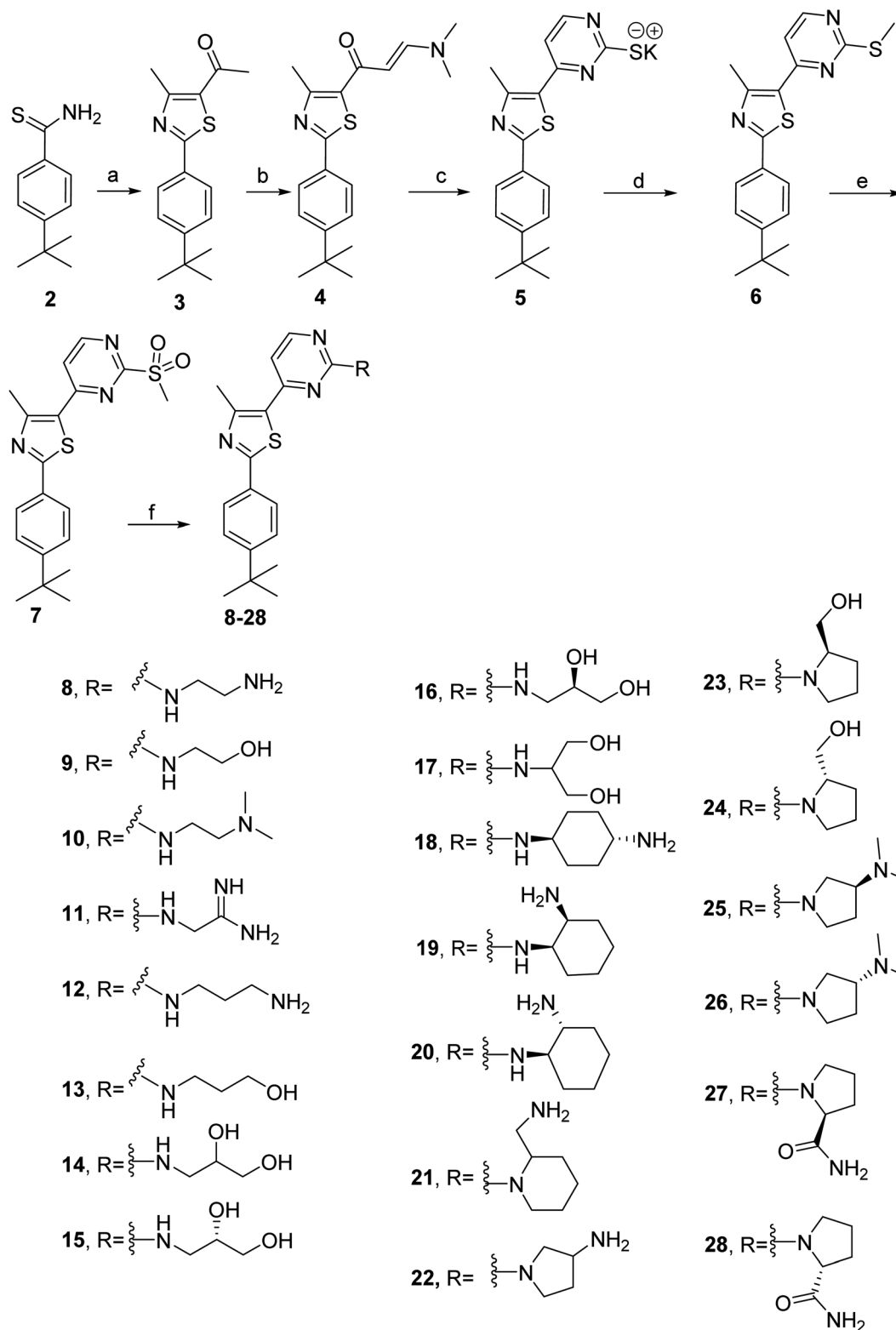
Previously, phenylthiazoles were reported to be new scaffolds with wide antimicrobial activity against multidrug-resistant strains of *S. aureus*, including MRSA and VRSA.²³ Deep-dive investigations on lead compound **1a** revealed its efficacy against bacteria arose from its ability to block the construction of their cell walls.²⁴ Prior to this finding, a thorough analysis of the structure–activity relationship (SAR) of **1a** showed that it possessed a central thiazole ring attached to two unique features: a cationic aminoguanidine moiety (highlighted in red in Fig. 1) at position C5 and a lipophilic *n*-butyl moiety (highlighted in blue) at C2. These two key features were vital for the potent activity against MRSA of **1a**, so removal of any one of them led to a complete loss of activity.²³ The bacterial target was not determined at the time of discovery of lead compound **1a**, so a structure-based drug-design approach could not be applied for further optimization of the structure. Instead, a lead compound-based

drug-design approach had been adopted and two important structural elements were identified: a guanidine moiety (colored red in Fig. 1) and a lipophilic tail (colored blue).²³

The initial series of phenylthiazole compounds (represented by compound **1a** in Fig. 1) suffered from a short half-life ($t_{1/2}$),²³ which limited systemic pharmacological application. A comprehensive metabolic study referred to the butyl benzylic carbon as a metabolic “soft spot”,²⁵ which replaced an oxygen atom to provide derivatives **1b** with a longer duration of action.²⁵ On the other hand, modifications related to the cationic head (where the readily hydrolysable C=N was incorporated in a heterocyclic linker system) led to the potent and metabolically stable analogue **1c** (Fig. 1).²⁶

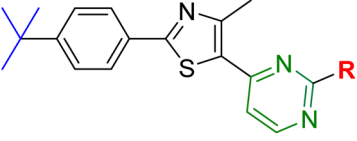
This structural modification of the cationic head resulted in several phenylthiazoles bearing, at thiazole position-5, a pyrimidine ring connected with different amines, guanidine, or a guanidine-like moiety.²⁶ A biological study of this generation indicated that cationic side chains with more than one





Scheme 1 Reagents and conditions: (a) absolute EtOH, 3-chloropentane-2,4-dione, heat at reflux, 12 h; (b) DMF–DMA heat at 80 °C, 8 h; (c) thiourea, KOH, EtOH, heat at reflux, 8 h; (d) dimethyl sulfate, KOH, H₂O, stirring at 23 °C, 2 h; (e) MCPBA, dry DCM, stirring at 23 °C, 16 h; (f) appropriate amine, dry DMF, heat at 80 °C for 0.5–8 h.

Table 1 The minimum inhibitory concentration (MIC; in $\mu\text{g mL}^{-1}$) of new synthesized pyrimidine derivatives and control drugs (gentamicin, linezolid, vancomycin, cefixime, amphotericin B, and fluconazole) initially screened against isolates of methicillin-resistant *Staphylococcus aureus*, *Clostridium difficile*, *Escherichia coli*, *Neisseria gonorrhoeae* and *Candida albicans*



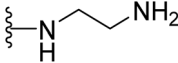
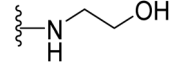
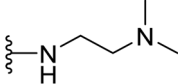
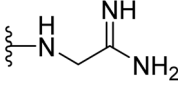
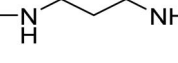
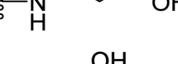
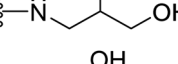
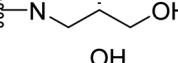
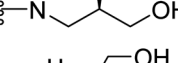
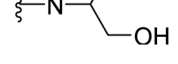
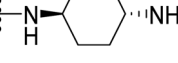
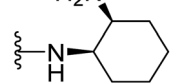
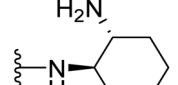
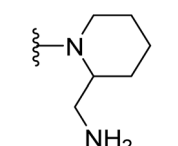
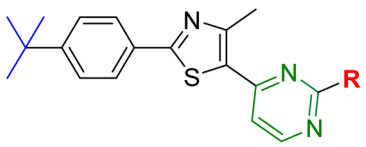
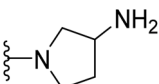
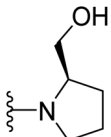
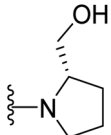
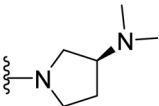
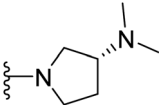
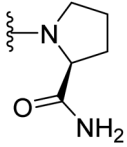
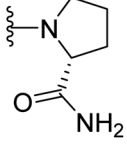
Cpd	Side chain	MRSA NRS384 (MRSA USA300)	<i>E. coli</i> JW55031 (TolC mutant)	<i>E. coli</i> BW25113 (wild-type strain)	<i>Clostridium</i> <i>difficile</i> ATCC BAA 1870	<i>Candida albicans</i> ATCC 64124	<i>Neisseria</i> <i>gonorrhoeae</i> 194
1a	NA	4.8	NT	NT	NT	NT	NT
8		>64	>64	>64	>64	64	>64
9		32	>64	>64	16	>64	>64
10		>64	>64	>64	32	64	>64
11		>64	>64	>64	>64	>64	>64
12		32	32	>64	16	8	>64
13		16	>64	>64	4	>64	>64
14		>64	>64	>64	16	>64	>64
15		32	>64	>64	16	>64	>64
16		32	>64	>64	8	>64	>64
17		>64	>64	>64	32	>64	>64
18		16	16	>64	32	16	>64
19		4	>64	>64	8	>64	>64
20		4	8	>64	4	4	>64
21		16	16	>64	8	16	>64



Table 1 (Contd.)



Cpd	Side chain	MRSA NRS384 (MRSA USA300)	<i>E. coli</i> JW55031 (TolC mutant)	<i>E. coli</i> BW25113 (wild-type strain)	<i>Clostridium</i> <i>difficile</i> ATCC BAA 1870	<i>Candida albicans</i> ATCC 64124	<i>Neisseria</i> <i>gonorrhoeae</i> 194
22		16	16	>64	>64	>64	>64
23		>64	>64	>64	32	>64	>64
24		>64	>64	>64	64	>64	>64
25		32	>64	>64	32	>64	>64
26		16	>64	>64	16	>64	>64
27		16	>64	>64	16	>64	>64
28		16	>64	>64	8	>64	>64
Linezolid	NA	1	8	>64		NT	NT
Vancomycin	NA	1	NT	NT		NT	NT
Gentamicin	NA	NT	≤0.5	≤0.5		NT	NT
Cefixime	NA	NT	NT	NT		NT	1
Amphotericin B	NA	NT	NT	NT		1	NT
Fluconazole	NA	NT	NT	NT		>64	NT

heteroatom (N or O) had greater antibacterial action, and drew attention to the role of the distance and configuration of this moiety upon activity (Fig. 1).²⁶

The present study investigated a dual tactic to maximize pharmacodynamic and pharmacokinetic profiles by blocking the metabolic soft spot (benzylic C–H oxidation) and preventing hydrolysis of the Schiff bond. The first tactic was achieved *via*

replacement of the *n*-butyl of lead compound **1a** with a tertiary isostere, whereas the second tactic was achieved by incorporating it in the rigid system (pyrimidine linker).^{26,27} In addition, the SAR at the nitrogenous head was studied carefully. A new set of derivatives was designed to cover all possibilities of the distance between the heteroatoms and/or different spatial configurations of the cationic head (Fig. 1).



2. Results and discussion

2.1. Chemistry

The methylsulfonyl derivative **7** was readily obtained, as reported previously,²⁸ by allowing enaminone **4** to react with thiourea followed by methylation with dimethyl sulfate and oxidation of the corresponding thioether **6** using *m*-chloroperbenzoic acid (MCPBA) (Scheme 1). In an attempt to use an alternative shorter pathway, enaminone **4** was allowed to react with *S*-methylisothiourea. Unfortunately, the required product (compound **6**) could not be separated from the reaction mixture with the desirable purity, and most of the yield was lost during successive chromatographic separations. The inserted *S*-methyl group of compound **6** was represented by one extra singlet signal in the aliphatic region of the ¹H NMR spectrum at 2.77 ppm. This signal was shifted downfield to 3.47 ppm upon oxidation of thioether **6** to the methylsulfonyl analogue **7**. Finally, the methylsulfonyl intermediate **7** was utilized to complete a series of optimized *tert*-butylphenylthiazoles. Hence, the methylsulfonyl moiety was reacted with 21 nucleophiles to afford the corresponding final products **8–28**, respectively (Scheme 1). These nucleophiles included primary and secondary amines. The structures of this set of novel compounds were confirmed by spectral and elemental analyses (see Experimental section).

2.2. Biological results and discussion

2.2.1 Initial antimicrobial assessment and establishing SAR. All synthesized compounds were subject to an initial filtration against microbes that included two Gram-positive, two Gram-negative strains, and one *Candida* species using the broth-microdilution method according to guidelines outlined by the Clinical and Laboratory Standards Institute.^{29–31}

Studying the antimicrobial activity of the newly synthesized compounds with a two-carbon unit distance between the two heteroatoms (compounds **8–14**) provided considerable SAR information. In brief, ethylenediamine-containing compound

8 did not have any microbial activity. Addition of two alkyl groups at the second nitrogen (compound **10**) resulted in an increase in antimicrobial activity against *C. difficile*. Replacement of the free amino group with a hydroxyl group provided (compound **9**) with one-fold enhanced antibacterial activity against *C. difficile* and weak activity against MRSA because the minimum inhibitory concentration (MIC) value of **9** was 32 µg mL^{−1} vs. MRSA and 16 µg mL^{−1} vs. *C. difficile*. The second set of structural optimizations included an increase in the distance to three carbon units to give compounds **12–16**. Propylenediamine derivative **12** maintained the antibacterial activity of compound **9** in addition to moderate antifungal activity with an MIC of 8 µg mL^{−1}. The hydroxyl analogue (compound **13**) was more potent than compound **12** with one-fold activity (MIC = 16 µg mL^{−1}) vs. MRSA and four-fold activity against *C. difficile* (MIC = 4 µg mL^{−1}). All other derivatives with a second hydroxyl group at the adjacent carbon with different chirality (stereoisomers **14**, **15**, **16** and **17**) maintained activity against Gram-positive bacteria. The only exceptions among the hydroxylated derivatives were the diol positional isomers **14** and **17**, which reduced the activity against *C. difficile* with MIC values of 16 and 32 µg mL^{−1}, respectively. This result suggested that compounds **14** and **17** might possess selective activity against Gram-positive bacteria or specifically *C. difficile*. This observation might add an additional clinical value because compounds **14** and **17** are not expected to disturb the normal human microbiota (Table 1).

Encouraged by the previous result, the next set of structures **18–28** included addition of a second polar atom (N or O) at a two-carbon-unit distance with different possibilities for spatial configurations. For the diamino-cyclohexane derivatives **18**, **19** and **20**, the *trans*-1,2-diamino isomer (compound **20**) showed good anti-MRSA activity with an MIC value of 4 µg mL^{−1} (near to that of the lead structure **1a**) in addition to potent activity against *C. difficile* and *Candida* species and moderate activity against Gram-negative bacteria. Changing the stereo

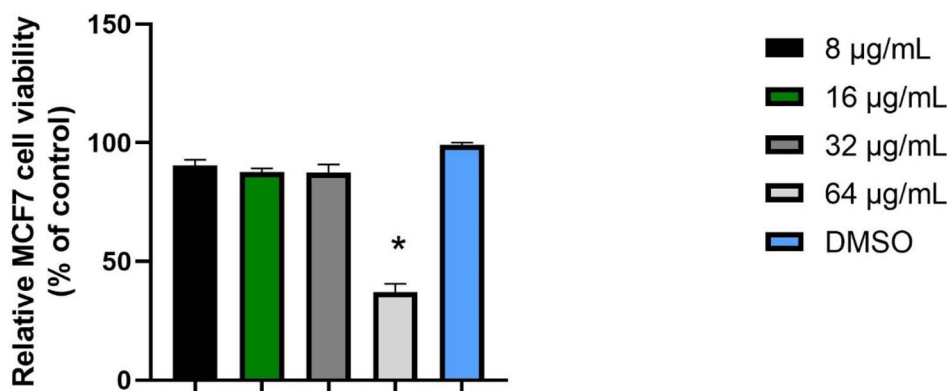


Fig. 2 Analyses of the toxicity of compound **20** (tested in triplicates at 8, 16, 32 and 64 µg mL^{−1}) against human breast cancer (MCF-7) cells using the 3-(4,5-dimethylthiazol-2-yl)-5-(3-carboxymethoxyphenyl)-2-(4-sulfophenyl)-2H-tetrazolium (MTS) assay. Results are presented as percent viable cells relative to DMSO (negative control) to determine a baseline measure for the cytotoxic impact of each compound. Absorbance values represent an average of three samples analyzed for each compound. Error bars represent standard deviation values. Data were analyzed via two-way ANOVA with *post hoc* Dunnett's test for multiple comparisons. * denotes a significant difference (*P* < 0.05) between values obtained for compounds and DMSO.



Table 2 Computational studies to reveal the molecular properties of compounds

Software		SWISS-ADME		DS ^a										SWISS-ADME			MolSoft	
Parameters																		
vs. compounds	GI absorption	CYP 1A2 inhibitor	CYP 2C19 inhibitor	CYP 2C9 inhibitor	CYP 2D6 inhibitor	CYP 3A4 inhibitor	CYP2D6 applicability MDp value	PPB availability	Hepatotoxic availability	Log <i>p</i> o/w	Alog <i>p</i>	Mol log <i>p</i>	p <i>K</i> _a (most basic/acidic groups)	Model score				
	Log <i>S</i>																	
	Solubility																	
Lead 1a	High	Yes	Yes	Yes	No	Yes	1.15996 × 10 ^{−5}	16.07	13.51	3.08	3.699	4.48	1.02	0.68				
Lead 1c	Low	Yes	Yes	Yes	No	Yes	5.20627 × 10 ^{−6}	15.45	11.71	3.25	4.339	4.44	0.82	1.47				
Comp. 20	High	No	Yes	No	No	Yes	1.63303 × 10 ^{−5}	13.07	10.82	4.20	4.325	5.34	0.81	0.68				

^a DS: Discovery Studio 4.1 software. ^b Mod.: moderate.

^a DS: Discovery Studio 4.1 software. ^b Mod.: moderate.

configuration of the two amino group to *cis* (compound **19**) maintained the anti-MRSA activity with an MIC value of 4 µg mL⁻¹ but decreased activity against tested *Escherichia coli*, *C. difficile*, and *Candida albicans* (Table 1). In addition, compound **18** (1,4-diamino isomer) maintained moderate potency against the *E. coli* JW55031 strain, MRSA USA300, and *C. albicans*.

On the other hand, pyrrolidine-containing derivatives **22–28** showed mixed effects against microbes. The amino pyrrolidine **22** had moderate activity against MRSA and *E. coli* JW55031 and showed a MIC value of 16 µg mL⁻¹, respectively. Hydroxymethylpyrrolidines **24** were completely void of antimicrobial activity. Carboximidine and dimethylamino pyrrolidine derivatives **25–28** showed moderate activity against MRSA and *C. difficile* strains.

In brief, our SAR study revealed the impact of structural modifications on the antimicrobial activity of newly synthesized compounds. Ethylenediamine (compound **8**) lacked activity, but addition of alkyl groups (compound **10**) or hydroxylation (compound **9**) enhanced activity against *C. difficile*. Increasing the carbon distance (compounds **12–16**) maintained activity, and introduction of a second polar atom (compounds **18–28**) enabled further elucidation of the SAR. Pyrrolidine-containing derivatives (compounds **22–28**) exhibited mixed effects. These findings provided valuable insights into the potential of these compounds as antimicrobial agents.

2.2.2 Toxicity profile. Assessment of the toxicity of new compounds with potential antibacterial activity is crucial to ensure their safety for host tissues. In the present study, compound **20** exhibited favorable toxicity profiles when tested on MCF-7 cells. Notably, even at high concentrations, compound **20** demonstrated remarkable tolerance by MCF-7 cells. Up to concentrations of 32 µg mL⁻¹ (8-fold of MIC), the compound maintained 100% cell viability, as evidenced by Fig. 2.

2.3. Absorption, distribution, metabolism, and excretion (ADME) studies

2.3.1 ADME calculations. Metabolic resistance of compound **20** was determined *via* computational studies compared with lead compounds **1a** and **1c**. Moreover, the bioavailability (*via* the permeability and penetration of bacterial membranes) was tested through log *p* calculations. Adopting the SWISS-ADME method, the three compounds were subjected to calculations of ADME molecular properties and count of cytochrome P450 (CYP) inhibition using five strains. The results are shown in Table 2, Fig. 3 and 4. The results were also validated using drug-likeness calculations to predict Mol log *p* for hydrophobicity comparison, pK_a, and model score of drug-likeness (Fig. 5).

The results shown above displayed clear evidence of low interaction of compound **20** with metabolic enzymes compared with that of the other two lead compounds, which suggested metabolic stability. Moreover, the hydrophobicity of compound **20** expressed in different forms of log *p* was higher than those of the lead compounds, which provided proof of efficient permeability and penetration of bacterial membranes, suggesting that it was a more bioavailable drug.



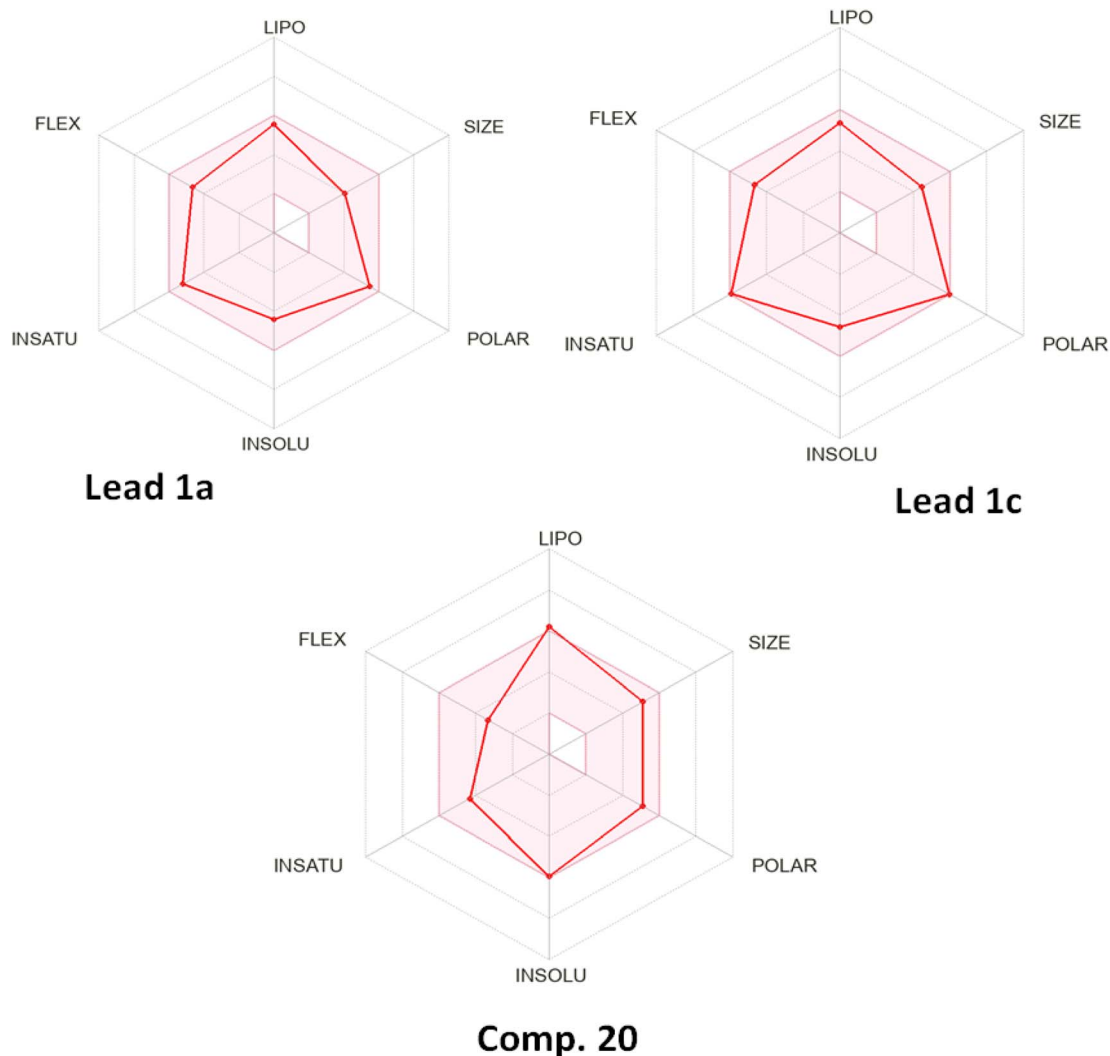


Fig. 3 Radar map of the ADME calculations for lead compound 1a, lead compound 1c, and compound 20.

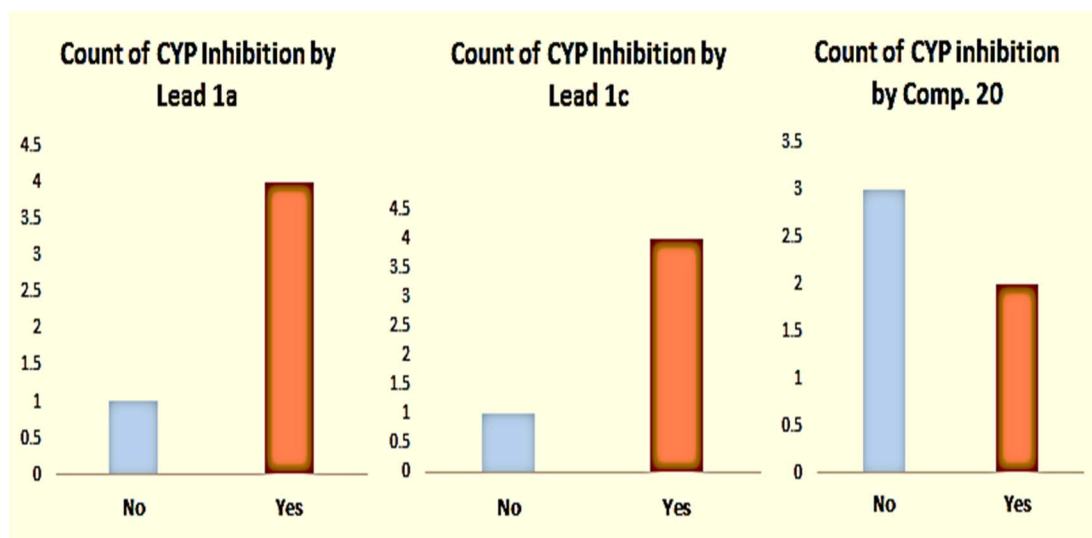


Fig. 4 Count of CYP inhibition of five strains by lead compound 1a, lead compound 1c, and compound 20.

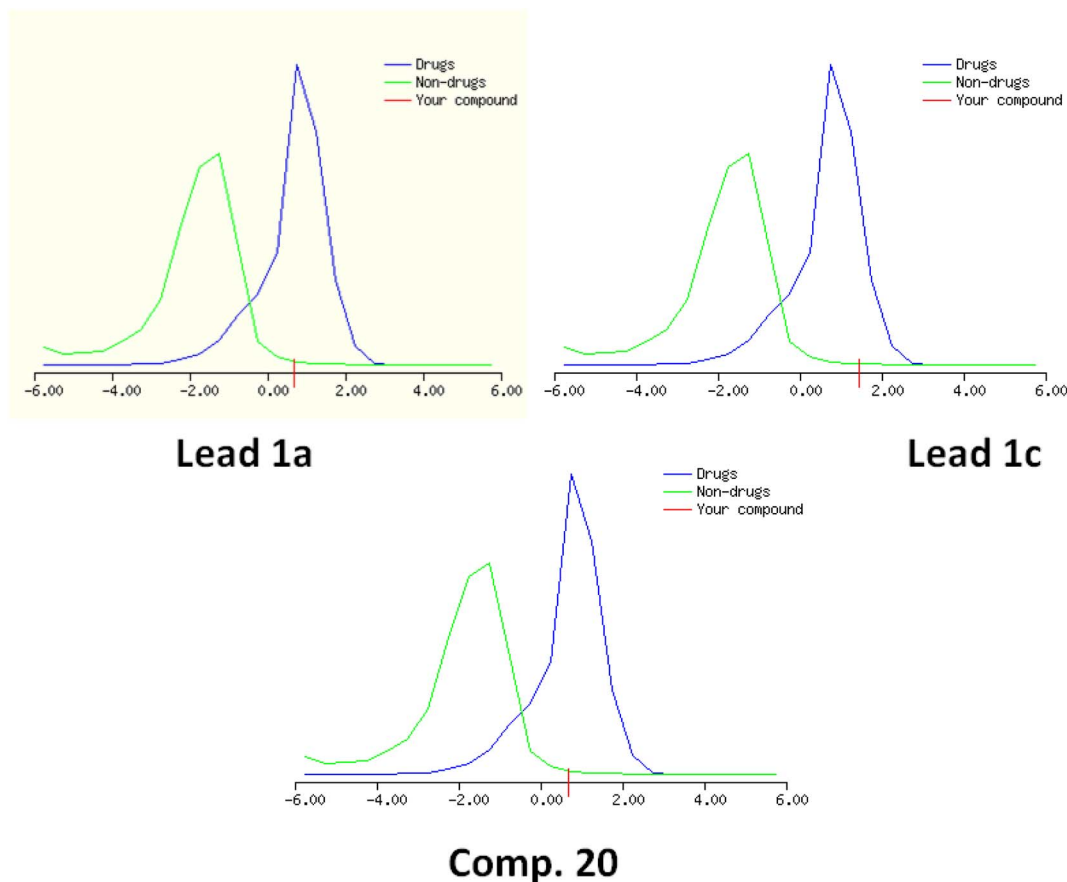


Fig. 5 Drug-likeness model obtained from calculations of molecular properties of lead compound 1a, lead compound 1c, and compound 20.

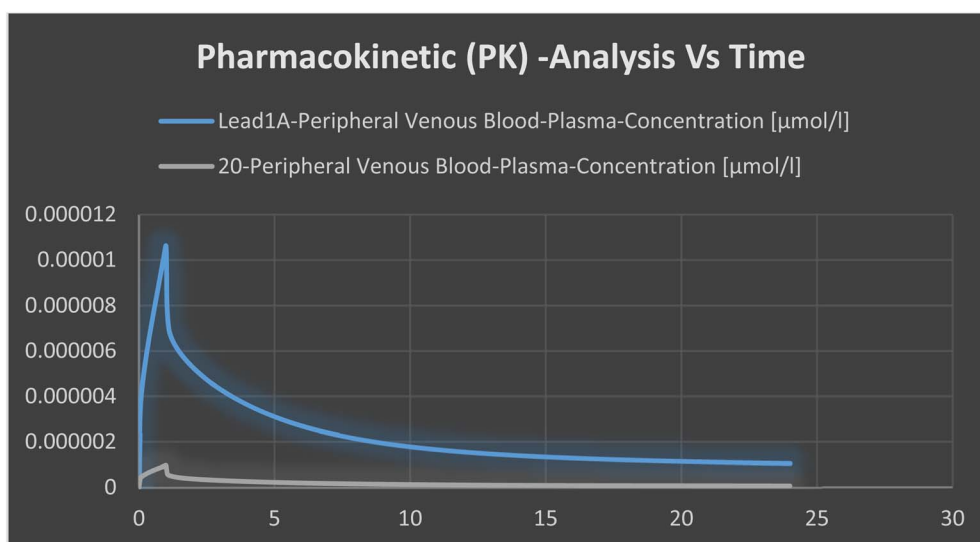


Fig. 6 Pharmacokinetic analysis of lead compound 1a and compound 20.

2.3.2 Metabolism simulation. We wished to assure the stability of compound 20 against metabolism. PK-Sim software was utilized to simulate metabolic and bioavailable processes within the human body. Different parameters were obtained from the pharmacokinetic analysis which reflected the

superiority of new compound 20 over its lead compound (Fig. 6). The most crucial parameter was the expected $t_{1/2}$ of the drug, which for lead compound 1a was estimated to be 20.455495 min and for compound 20 was 21.604437 min (Fig. 7). Thus, new compound 20 could have certain metabolic

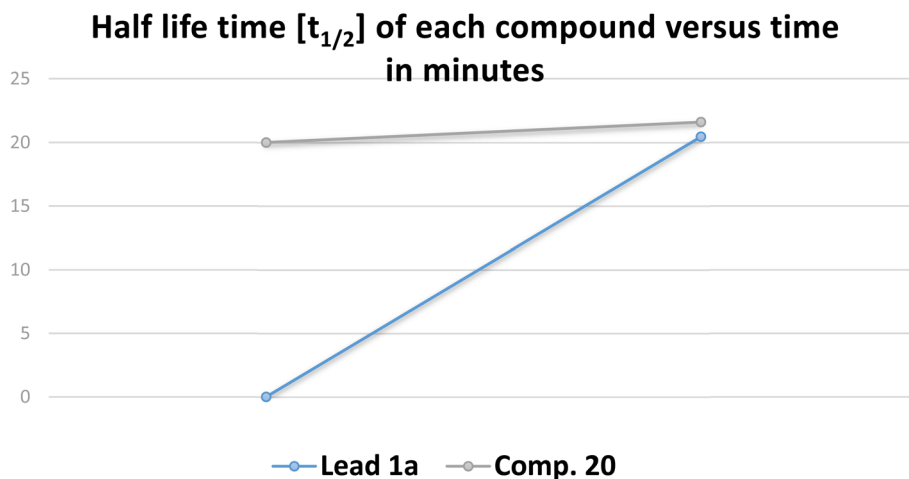


Fig. 7 Half-life of lead compound **1a** and compound **20**.

resistance and greater penetration of membranes for treating MRSA.

Owing to the tertiary butyl group rather than an *n*-alkyl chain, the hydrophobicity of compound **20** was higher and penetration of bacterial membranes was greater. Also, the bulky steric effect of the group hindered the metabolic process, so a longer duration of biological activity was observed.^{32,33}

3. Conclusions

Dual modification on lead compound **1a** (via a *t*-butyl moiety and pyrimidine linker) provided a new series of phenylthiazoles characterized by broad-spectrum antimicrobial activity. Among the tested nitrogenous moieties, compounds **19** and **20**, with a two-carbon distance between the two hetero atoms through a six-membered ring, possessed the most potent activity against the highly infectious MRSA USA300 strain with an MIC value of 4 $\mu\text{g mL}^{-1}$. Compounds **13** and **20** exhibited potent activity against *C. difficile*. Four other derivatives (**16**, **19**, **21**, and **28**) exhibited moderate activity against *C. difficile* with MIC values of 8 $\mu\text{g mL}^{-1}$, respectively. Compounds **20**, **21**, and **22** exhibited some activity against TolC-mutant *E. coli*, and they did not show activity against wild-type *E. coli* nor *N. gonorrhoeae*, suggesting that these compounds might be removed from Gram-negative bacteria by efflux pumps. Also, compounds **12**, **18**, **20**, and **21** exhibited activity against a *C. albicans* strain with MIC values of 4–16 $\mu\text{g mL}^{-1}$.

4. Experimental

4.1. Chemistry

4.1.1 General. ^1H NMR spectroscopy was undertaken at 400 MHz. ^{13}C spectra were determined at 100 MHz in deuterated dimethyl sulfoxide ($\text{DMSO}-d_6$) on a Varian Mercury VX-400 NMR spectrometer. Chemical shifts are given in parts per million (ppm) on the delta (δ) scale. Chemical shifts were calibrated relative to those of solvents. Flash chromatography was performed on silica (230–400 mesh). The progress of reactions was

monitored with silica gel IB2-F plates of thickness 0.25 mm (Merck). Mass spectra were recorded at 70 eV. High-resolution mass spectra for all ionization methods were obtained from a Finnigan MAT XL95 setup. Melting points were determined using capillary tubes with a Stuart SMP30 apparatus and are uncorrected. All yields reported refer to isolated yields.

4.1.2 Compounds 8–28

General procedure. An appropriate amine (0.4 mmol) was added to a solution of compound **7** (0.1 g, 0.25 mmol) in dry DMF (5 mL). The reaction mixture was heated at 80 $^{\circ}\text{C}$ for 4–8 h, and then poured over iced water (50 mL). The formed solid was filtered and washed with 50% ethanol and recrystallized from absolute ethanol or extracted by ethyl acetate. Then, it was dried over MgSO_4 and evaporated under reduced pressure to give the products. The physical properties and spectral analysis of isolated products are shown below.

N-(4-[2-(4-(*tert*-Butyl)phenyl)-4-methylthiazol-5-yl]pyrimidin-2-yl)ethane-1,2-diamine (**8**). Following the general procedure and using ethylenediamine (21 μL , 0.4 mmol), compound **8** was obtained as a yellowish-brown solid (90 mg, 91%) mp = 137 $^{\circ}\text{C}$; ^1H NMR ($\text{DMSO}-d_6$) δ : 8.32 (d, J = 5.2 Hz, 1H), 7.86 (d, J = 7.6 Hz, 2H), 7.48 (d, J = 7.6 Hz, 2H), 7.11 (brs, 1H), 6.85 (d, J = 5.2 Hz, 1H), 3.48–3.45 (m, 2H), 2.72 (s, 3H), 2.58 (t, J = 12 Hz, 2H), 1.64 (brs, 1H), 1.30 (s, 9H); ^{13}C NMR ($\text{DMSO}-d_6$) δ : 166.6, 162.1, 159.0, 158.3, 154.1, 153.1, 131.6, 130.5, 126.5, 126.4, 106.5, 56.5, 44.4, 35.1, 31.3, 18.7; MS (m/z) 367; anal. calc. for: ($\text{C}_{20}\text{H}_{25}\text{N}_5$, Mwt = 367): C, 65.36; H, 6.86; N, 19.06; found: C, 65.46; H, 6.94; N, 19.11%.

2-[(4-[2-(4-(*tert*-Butyl)phenyl)-4-methylthiazol-5-yl]pyrimidin-2-yl)amino]ethan-1-ol (**9**). Following the general procedure and using 2-aminoethan-1-ol (21 μL , 0.4 mmol), compound **9** was obtained as yellowish-white solid (90 mg, 92%) mp = 123 $^{\circ}\text{C}$; ^1H NMR ($\text{DMSO}-d_6$) δ : 8.35 (d, J = 5.2 Hz, 1H), 7.89 (d, J = 7.6 Hz, 2H), 7.53 (d, J = 7.6 Hz, 2H), 7.11 (brs, 1H), 6.89 (d, J = 5.2 Hz, 1H), 4.68 (brs, 2H), 3.65 (d, J = 8 Hz, 2H), 3.54 (d, J = 8 Hz, 2H), 2.70 (s, 3H), 1.30 (s, 9H); ^{13}C NMR ($\text{DMSO}-d_6$) δ : 166.6, 162.1, 159.7, 157.9, 154.2, 153.8, 131.6, 130.5, 126.5, 126.4, 106.5, 60.1, 43.4, 35.1, 31.3, 18.7; MS (m/z) 368; anal. calc. for: ($\text{C}_{20}\text{H}_{24}\text{N}_4\text{O}_2\text{S}$,



Mwt = 368): C, 65.19; H, 6.57; N, 15.20; found: C, 65.27; H, 6.65; N, 15.26%.

N-{4-[2-(4-(*tert*-Butyl)phenyl)-4-methylthiazol-5-yl]pyrimidin-2-yl}-*N,N*-dimethylethane-1,2-diamine (**10**). Following the general procedure and using *N,N*-dimethylenediamine (32 μ L, 0.4 mmol), compound **10** was obtained as yellow solid (90 mg, 91%) mp = 117 $^{\circ}$ C; 1 H NMR (DMSO- d_6) δ : 8.33 (d, J = 5.2 Hz, 1H), 7.87 (d, J = 7.6 Hz, 2H), 7.53 (d, J = 7.6 Hz, 2H), 7.04 (brs, 1H), 6.88 (d, J = 5.2 Hz, 1H), 3.42–3.38 (m, 2H), 2.70 (s, 3H), 2.41 (t, J = 8 Hz, 2H), 2.18 (s, 6H), 1.28 (s, 9H); 13 C NMR (DMSO- d_6) δ : 166.6, 162.4, 160.7, 159.4, 154.0, 153.4, 131.6, 130.5, 126.5, 126.4, 106.5, 58.4, 45.7, 44.7, 35.1, 31.3, 18.6; MS (m/z) 395; anal. calc. for: (C₂₂H₂₉N₅S, Mwt = 395): C, 66.80; H, 7.39; N, 17.70; found: C, 66.89; H, 7.45; N, 17.77%.

2-[[4-(2-(4-(*tert*-Butyl)phenyl)-4-methylthiazol-5-yl)pyrimidin-2-yl]amino]acetimidamide (**11**). Following the general procedure and using 2-aminoacetimidamide dihydrobromide (90 mg, 0.4 mmol) and anhydrous potassium carbonate (0.1 g, 0.7 mmol), compound **11** was obtained as a brown solid (70 mg, 74%) mp = 189 $^{\circ}$ C; 1 H NMR (DMSO- d_6) δ : 8.73 (brs, 2H), 8.32 (d, J = 5.2 Hz, 1H), 7.83 (d, J = 7.6 Hz, 2H), 7.53 (d, J = 7.6 Hz, 2H), 6.90 (d, J = 5.2 Hz, 1H), 6.68 (brs, 2H), 3.19 (s, 2H), 2.68 (s, 3H), 1.29 (s, 9H); 13 C NMR (DMSO- d_6) δ : 166.6, 163.7, 159.6, 159.0, 158.3, 153.9, 153.5, 131.6, 130.5, 126.5, 126.4, 106.9, 45.1, 39.3, 35.1, 31.3, 18.6; MS (m/z) 380; anal. calc. for: (C₂₀H₂₄N₆S, Mwt = 380): C, 63.13; H, 6.36; N, 22.09; found: C, 63.21; H, 6.43; N, 22.19%.

N-{4-[2-(4-(*tert*-Butyl)phenyl)-4-methylthiazol-5-yl]pyrimidin-2-yl}propane-1,3-diamine (**12**). Following the general procedure and using propane-1,3-diamine (27 μ L, 0.4 mmol), compound **12** was obtained as a buff solid (91 mg, 89%) mp = 165 $^{\circ}$ C; 1 H NMR (DMSO- d_6) δ : 8.36 (d, J = 5.2 Hz, 1H), 7.89 (d, J = 7.6 Hz, 2H), 7.53 (d, J = 7.6 Hz, 2H), 7.33 (brs, 1H), 6.87 (d, J = 5.2 Hz, 1H), 3.45–3.41 (m, 2H), 2.70 (s, 3H), 2.63 (t, J = 12 Hz, 2H), 1.66 (brs, 2H), 1.30 (s, 9H), 1.15–1.13 (m, 2H); 13 C NMR (DMSO- d_6) δ : 166.3, 159.0, 158.2, 157.2, 154.5, 153.1, 131.6, 130.5, 126.7, 126.4, 106.5, 46.1, 45.1, 34.3, 32.3, 31.2, 18.7; MS (m/z) 381; anal. calc. for: (C₂₁H₂₇N₅S, Mwt = 381): C, 66.11; H, 7.13; N, 18.36; found: C, 66.17; H, 7.19; N, 18.43%.

3-[[4-(2-(4-(*tert*-Butyl)phenyl)-4-methylthiazol-5-yl)pyrimidin-2-yl]amino]propan-1-ol (**13**). Following the general procedure and using 3-aminopropan-1-ol (27 μ L, 0.4 mmol), compound **13** was obtained as a yellowish-brown solid (93 mg, 83%) mp = 110 $^{\circ}$ C; 1 H NMR (DMSO- d_6) δ : 8.33 (d, J = 5.2 Hz, 1H), 7.88 (d, J = 7.6 Hz, 2H), 7.53 (d, J = 7.6 Hz, 2H), 7.19 (brs, 1H), 6.87 (d, J = 5.2 Hz, 1H), 4.45 (brs, 1H), 3.50–3.35 (m, 4H), 2.69 (s, 3H), 1.73–1.67 (m, 2H), 1.29 (s, 9H); 13 C NMR (DMSO- d_6) δ : 166.6, 162.5, 159.4, 157.6, 154.0, 153.4, 131.9, 130.5, 126.5, 126.4, 106.5, 59.2, 38.5, 35.1, 32.5, 31.3, 18.6; MS (m/z) 382; anal. calc. for: (C₂₁H₂₆N₄OS, Mwt = 382): C, 65.94; H, 6.85; N, 14.65; found: C, 66.01; H, 6.93; N, 14.74%.

3-[[4-(2-(4-(*tert*-Butyl)phenyl)-4-methylthiazol-5-yl)pyrimidin-2-yl]amino]propane-1,2-diol (**14**). Following the general procedure and using 3-aminopropane-1,2-diol (33 μ L, 0.4 mmol), compound **14** was obtained as a yellowish-white solid (72 mg, 63%) mp = 106 $^{\circ}$ C; 1 H NMR (DMSO- d_6) δ : 8.32 (d, J = 5.2 Hz, 1H), 7.87 (d, J = 7.6 Hz, 2H), 7.51 (d, J = 7.6 Hz, 2H), 6.99 (brs, 1H), 6.86 (d, J = 5.2 Hz, 1H), 4.81 (brs, 1H), 4.59 (brs, 1H), 3.73–

3.61 (m, 1H), 3.47–3.42 (m, 2H), 3.27–3.21 (m, 2H), 2.69 (s, 3H), 1.28 (s, 9H); 13 C NMR (DMSO- d_6) δ : 166.7, 162.5, 159.4, 158.5, 154.0, 153.5, 131.7, 130.5, 126.4, 126.0, 106.8, 70.6, 64.5, 44.7, 35.0, 31.3, 18.6; MS (m/z) 398; anal. calc. for: (C₂₁H₂₆N₄O₂S, Mwt = 398): C, 63.29; H, 6.58; N, 14.06; found: C, 63.35; H, 6.66; N, 14.11%.

(*R*)-3-[[4-[2-(4-(*tert*-Butyl)phenyl)-4-methylthiazol-5-yl]pyrimidin-2-yl]amino]propane-1,2-diol (**15**). Following the general procedure and using (*R*)-3-aminopropane-1,2-diol (33 mg, 0.4 mmol), compound **15** was obtained as a brown solid (60 mg, 57%) mp = 166 $^{\circ}$ C; 1 H NMR (DMSO- d_6) δ : 8.34 (d, J = 5.2 Hz, 1H), 7.86 (d, J = 7.6 Hz, 2H), 7.52 (d, J = 7.6 Hz, 2H), 6.99 (brs, 1H), 6.87 (d, J = 5.2 Hz, 1H), 4.77 (brs, 1H), 4.54 (brs, 1H), 3.73–3.60 (m, 1H), 3.47–3.41 (m, 2H), 3.27–3.21 (m, 2H), 2.69 (s, 3H), 1.29 (s, 9H); 13 C NMR (DMSO- d_6) δ : 166.6, 162.5, 159.3, 158.7, 154.0, 153.5, 131.6, 130.5, 126.8, 126.4, 106.8, 70.6, 64.5, 44.8, 35.1, 30.5, 18.6; MS (m/z) 398; anal. calc. for: (C₂₁H₂₆N₄O₂S, Mwt = 398): C, 63.29; H, 6.58; N, 14.06; found: C, 63.37; H, 6.68; N, 14.10%.

(*S*)-3-[[4-[2-(4-(*tert*-Butyl)phenyl)-4-methylthiazol-5-yl]pyrimidin-2-yl]amino]propane-1,2-diol (**16**). Following the general procedure and using (*S*)-3-aminopropane-1,2-diol (33 mg, 0.4 mmol), compound **16** was obtained as a yellow solid (73 mg, 75%) mp = 159 $^{\circ}$ C; 1 H NMR (DMSO- d_6) δ : 8.33 (d, J = 5.2 Hz, 1H), 7.85 (d, J = 7.6 Hz, 2H), 7.51 (d, J = 7.6 Hz, 2H), 6.98 (brs, 1H), 6.87 (d, J = 5.2 Hz, 1H), 4.78 (brs, 1H), 4.57 (brs, 1H), 3.74–3.61 (m, 1H), 3.53–3.46 (m, 2H), 3.26–3.22 (m, 2H), 2.69 (s, 3H), 1.28 (s, 9H); 13 C NMR (DMSO- d_6) δ : 166.7, 162.1, 159.4, 158.2, 154.0, 153.5, 131.7, 130.5, 126.4, 126.0, 106.8, 70.6, 64.5, 44.7, 37.1, 31.3, 18.6; MS (m/z) 398; anal. calc. for: (C₂₁H₂₆N₄O₂S, Mwt = 398): C, 63.29; H, 6.58; N, 14.06; found: C, 63.38; H, 6.68; N, 14.11%.

2-[[4-(2-(4-(*tert*-Butyl)phenyl)-4-methylthiazol-5-yl)pyrimidin-2-yl]amino]propane-1,3-diol (**17**). Following the general procedure and using 2-aminopropane-1,3-diol (33 mg, 0.4 mmol), compound **17** was obtained as a yellow solid (80 mg, 81%) mp = 154 $^{\circ}$ C; 1 H NMR (DMSO- d_6) δ : 8.34 (d, J = 5.2 Hz, 1H), 7.88 (d, J = 7.6 Hz, 2H), 7.52 (d, J = 7.6 Hz, 2H), 6.89 (d, J = 5.2 Hz, 1H), 6.66 (brs, 1H), 4.63 (brs, 2H), 3.97–3.93 (m, 1H), 3.61–3.59 (m, 4H), 2.69 (s, 3H), 1.29 (s, 9H); 13 C NMR (DMSO- d_6) δ : 166.6, 162.3, 159.2, 157.9, 154.0, 153.5, 131.7, 130.5, 126.0, 125.7, 106.9, 60.6, 55.0, 35.1, 30.8, 18.7; MS (m/z) 398; anal. calc. for: (C₂₁H₂₆N₄O₂S, Mwt = 398): C, 63.29; H, 6.58; N, 14.06; found: C, 63.37; H, 6.67; N, 14.12%.

N-{4-[2-(4-(*tert*-Butyl)phenyl)-4-methylthiazol-5-yl]pyrimidin-2-yl}cyclohexane-*trans*-1,4-diamine (**18**). Following the general procedure and using *trans*-1,4-diaminocyclohexane (42 mg, 0.4 mmol), compound **18** was obtained as a brown solid (100 mg, 92%) mp = 193 $^{\circ}$ C; 1 H NMR (DMSO- d_6) δ : 8.31 (d, J = 5.2 Hz, 1H), 7.87 (d, J = 7.6 Hz, 2H), 7.56 (d, J = 7.6 Hz, 2H), 7.10 (brs, 1H), 6.91 (d, J = 5.2 Hz, 1H), 3.67–3.64 (m, 2H), 2.69 (s, 3H), 2.0–1.79 (m, 4H), 1.60 (brs, 2H), 1.29 (s, 9H) 1.20 (m, 4H); 13 C NMR (DMSO- d_6) δ : 166.3, 161.8, 159.7, 157.6, 154.0, 153.8, 131.9, 130.5, 126.5, 126.4, 106.5, 54.8, 50.1, 36.9, 35.1, 34.6, 31.3, 18.5; MS (m/z) 421; anal. calc. for: (C₂₄H₃₁N₅S, Mwt = 421): C, 68.37; H, 7.41; N, 16.61; found: C, 68.43; H, 7.47; N, 16.67.

N-{4-[2-(4-(*tert*-Butyl)phenyl)-4-methylthiazol-5-yl]pyrimidin-2-yl}cyclohexane-*cis*-1,2-diamine (**19**). Following the general procedure and using (±)-*cis*-1,2-diaminocyclohexane (42 µL, 0.4 mmol), compound **19** was obtained as a brown solid (71 mg, 62%) mp = 116 °C; ¹H NMR (DMSO-*d*₆) δ: 8.33 (d, *J* = 5.2 Hz, 1H), 7.82 (d, *J* = 7.6 Hz, 2H), 7.46 (d, *J* = 7.6 Hz, 2H), 6.82 (d, *J* = 5.2 Hz, 1H), 5.60 (brs, 1H), 3.99–3.93 (m, 2H), 2.67 (s, 3H), 1.95–1.38 (m, 8H), 1.26 (s, 9H), 1.60 (brs, 2H); ¹³C NMR (DMSO-*d*₆) δ: 166.6, 159.5, 159.1, 157.8, 153.8, 153.4, 131.6, 130.5, 126.4, 126.0, 105.9, 62.4, 54.8, 37.2, 35.0, 31.2, 26.4, 22.5, 19.7, 18.7; MS (*m/z*) 421; anal. calc. for: (C₂₄H₃₁N₅S, Mwt = 421): C, 68.37; H, 7.41; N, 16.61; found: C, 68.45; H, 7.45; N, 16.66.

N-{4-[2-(4-(*tert*-Butyl)phenyl)-4-methylthiazol-5-yl]pyrimidin-2-yl}cyclohexane-*trans*-1,2-diamine (**20**). Following the general procedure and using (±)-*trans*-1,2-diaminocyclohexane (42 µL, 0.4 mmol), compound **20** was obtained as a brown solid (100 mg, 89%) mp = 111 °C; ¹H NMR (DMSO-*d*₆) δ: 8.31 (d, *J* = 5.2 Hz, 1H), 7.86 (d, *J* = 7.6 Hz, 2H), 7.53 (d, *J* = 7.6 Hz, 2H), 7.11 (brs, 1H), 6.88 (d, *J* = 5.2 Hz, 1H), 3.48–3.43 (m, 2H), 2.68 (s, 3H), 2.05–1.86 (m, 3H), 1.64 (brs, 2H), 1.30 (s, 9H), 1.22–1.05 (m, 5H); ¹³C NMR (DMSO-*d*₆) δ: 166.6, 162.1, 159.0, 157.2, 154.0, 153.5, 131.9, 130.5, 126.5, 126.4, 106.5, 61.4, 54.2, 37.1, 35.1, 31.3, 25.3, 22.5, 19.7, 18.6; MS (*m/z*) 421; anal. calc. for: (C₂₄H₃₁N₅S, Mwt = 421): C, 68.37; H, 7.41; N, 16.61; found: C, 68.44; H, 7.46; N, 16.64.

4-[2-(4-(*tert*-Butyl)phenyl)-4-methylthiazol-5-yl]-*N*-(pyrrolidin-3-yl)pyrimidin-2-amine (**21**). Following the general procedure and using 3-amino-pyrrolidine dihydrochloride (60 mg, 0.4 mmol) and anhydrous potassium carbonate (0.1 g, 0.7 mmol), compound **21** was obtained as yellowish white solid (100 mg, 94%) mp = 115 °C; ¹H NMR (DMSO-*d*₆) δ: 8.41 (d, *J* = 5.2 Hz, 1H), 8.0 (brs, 1H), 7.89 (d, *J* = 7.6 Hz, 2H), 7.52 (d, *J* = 7.6 Hz, 2H), 6.90 (d, *J* = 5.2 Hz, 1H), 3.66–3.48 (m, 3H), 2.71 (s, 3H), 2.09–2.08 (m, 2H), 1.88 (brs, 1H), 1.73–1.70 (m, 2H), 1.30 (s, 9H); ¹³C NMR (DMSO-*d*₆) δ: 166.6, 160.1, 159.2, 158.0, 154.0, 153.4, 131.6, 130.5, 126.5, 126.4, 106.1, 54.5, 51.0, 45.2, 35.1, 33.6, 31.3, 18.6; MS (*m/z*) 393; anal. calc. for: (C₂₂H₂₇N₅S, Mwt = 393): C, 67.14; H, 6.92; N, 17.80; found: C, 67.22; H, 6.99; N, 17.87%.

4-[2-(4-(*tert*-Butyl)phenyl)-4-methylthiazol-5-yl]-*N*-(piperidin-2-ylmethyl)pyrimidin-2-amine (**22**). Following the general procedure and using 2-(aminomethyl)piperidine (42 µL, 0.4 mmol), compound **22** was obtained as a yellow solid (99 mg, 90%) mp = 146 °C; ¹H NMR (DMSO-*d*₆) δ: 8.33 (d, *J* = 5.2 Hz, 1H), 7.88 (d, *J* = 7.6 Hz, 2H), 7.53 (d, *J* = 7.6 Hz, 2H), 7.21 (brs, 1H), 6.88 (d, *J* = 5.2 Hz, 1H), 4.01–3.98 (m, 1H), 3.18–3.14 (m, 2H), 2.95–2.87 (m, 2H), 2.70 (s, 3H), 1.75–1.44 (m, 6H), 1.26 (s, 9H) 1.04 (brs, 1H); ¹³C NMR (DMSO-*d*₆) δ: 166.6, 162.6, 159.7, 159.0, 154.0, 153.4, 131.6, 130.5, 126.7, 126.4, 106.7, 70.1, 60.7, 56.1, 46.5, 35.1, 31.3, 26.2, 24.5, 18.6; MS (*m/z*) 421; anal. calc. for: (C₂₄H₃₁N₅S, Mwt = 421): C, 68.37; H, 7.41; N, 16.61; found: C, 68.44; H, 7.48; N, 16.66.

(*R*)-{1-[4-(2-(4-(*tert*-Butyl)phenyl)-4-methylthiazol-5-yl)pyrimidin-2-yl]pyrrolidin-2-yl}methanol (**23**). Following the general procedure and using (*R*)-(+)-2-pyrrolidinemethanol (37 µL, 0.4 mmol), compound **23** was obtained as a yellowish-green solid (90 mg, 85%) mp = 136 °C; ¹H NMR (DMSO-*d*₆) δ: 8.39 (d, *J*

= 5.2 Hz, 1H), 7.89 (d, *J* = 7.6 Hz, 2H), 7.53 (d, *J* = 7.6 Hz, 2H), 6.92 (d, *J* = 5.2 Hz, 1H), 4.85 (brs, 1H), 4.18–4.08 (m, 2H), 3.67–3.60 (m, 1H), 3.46–3.34 (m, 2H), 2.71 (s, 3H), 2.05–1.86 (m, 4H), 1.29 (s, 9H); ¹³C NMR (DMSO-*d*₆) δ: 166.6, 160.2, 159.4, 158.3, 154.0, 153.8, 131.9, 130.5, 126.5, 126.4, 106.3, 61.8, 59.0, 47.7, 35.1, 31.3, 28.1, 22.9, 18.6; MS (*m/z*) 408; anal. calc. for: (C₂₃H₂₈N₄OS, Mwt = 408): C, 67.62; H, 6.91; N, 13.71; found: C, 67.69; H, 6.97; N, 13.75%.

(*S*)-{1-[4-(2-(4-(*tert*-Butyl)phenyl)-4-methylthiazol-5-yl)pyrimidin-2-yl]pyrrolidin-2-yl}methanol (**24**). Following the general procedure and using (*S*)-(–)-2-pyrrolidinemethanol (37 µL, 0.4 mmol), compound **24** was obtained as a brown solid (100 mg, 96%) mp = 125 °C; ¹H NMR (DMSO-*d*₆) δ: 8.39 (d, *J* = 5.2 Hz, 1H), 7.88 (d, *J* = 7.6 Hz, 2H), 7.52 (d, *J* = 7.6 Hz, 2H), 6.89 (d, *J* = 5.2 Hz, 1H), 4.75 (brs, 1H), 4.18–4.12 (m, 2H), 3.67–3.63 (m, 1H), 3.52–3.46 (m, 2H), 2.69 (s, 3H), 2.03–1.89 (m, 4H), 1.29 (s, 9H); ¹³C NMR (DMSO-*d*₆) δ: 166.6, 160.2, 160.1, 159.0, 154.0, 153.4, 131.6, 130.5, 126.5, 126.4, 106.3, 61.1, 59.4, 47.4, 35.1, 31.3, 28.0, 23.2, 18.7; MS (*m/z*) 408; anal. calc. for: (C₂₃H₂₈N₄OS, Mwt = 408): C, 67.62; H, 6.91; N, 13.71; found: C, 67.70; H, 6.99; N, 13.77%.

(*R*)-1-[4-(2-(4-(*tert*-Butyl)phenyl)-4-methylthiazol-5-yl)pyrimidin-2-yl]-*N,N*-dimethylpyrrolidin-3-amine (**25**). Following the general procedure and using (*R*)-(+)-3-(dimethylamino)pyrrolidine dihydrochloride (71 mg, 0.4 mmol) and anhydrous potassium carbonate (0.1 g, 0.7 mmol), compound **25** was obtained as a yellow solid (99 mg, 91%) mp = 127 °C; ¹H NMR (DMSO-*d*₆) δ: 8.38 (d, *J* = 5.2 Hz, 1H), 7.89 (d, *J* = 7.6 Hz, 2H), 7.55 (d, *J* = 7.6 Hz, 2H), 6.93 (d, *J* = 5.2 Hz, 1H), 3.82–3.69 (m, 4H), 3.14–3.10 (m, 1H), 2.72 (s, 3H), 2.19 (s, 6H), 1.82–1.78 (m, 2H), 1.32 (s, 9H); ¹³C NMR (DMSO-*d*₆) δ: 166.6, 159.9, 159.2, 158.0, 154.0, 153.7, 131.5, 130.5, 126.5, 126.4, 106.3, 64.9, 50.3, 45.9, 44.2, 35.1, 31.3, 28.8, 18.7; MS (*m/z*) 421; anal. calc. for: (C₂₄H₃₁N₅S, Mwt = 421): C, 68.37; H, 7.41; N, 16.61; found: C, 68.42; H, 7.48; N, 16.65%.

(*S*)-1-[4-(2-(4-(*tert*-Butyl)phenyl)-4-methylthiazol-5-yl)pyrimidin-2-yl]-*N,N*-dimethylpyrrolidin-3-amine (**26**). Following the general procedure and using (*S*)-(–)-3-(dimethylamino)pyrrolidine (42 µL, 0.4 mmol), compound **26** was obtained as a yellow solid (81 mg, 73%) mp = 136 °C; ¹H NMR (DMSO-*d*₆) δ: 8.35 (d, *J* = 5.2 Hz, 1H), 7.84 (d, *J* = 7.6 Hz, 2H), 7.51 (d, *J* = 7.6 Hz, 2H), 6.88 (d, *J* = 5.2 Hz, 1H), 3.74–3.66 (m, 4H), 3.19–3.17 (m, 1H), 2.69 (s, 3H), 2.17 (s, 6H), 1.77–1.70 (m, 2H), 1.28 (s, 9H); ¹³C NMR (DMSO-*d*₆) δ: 166.6, 159.8, 159.1, 158.0, 153.9, 153.7, 131.4, 130.5, 126.7, 126.4, 106.2, 56.1, 50.9, 45.9, 44.2, 35.0, 31.3, 29.7, 18.7; MS (*m/z*) 421; anal. calc. for: (C₂₄H₃₁N₅S, Mwt = 421): C, 68.37; H, 7.41; N, 16.61; found: C, 68.42; H, 7.46; N, 16.67%.

(*S*)-1-[4-(2-(4-(*tert*-Butyl)phenyl)-4-methylthiazol-5-yl)pyrimidin-2-yl]pyrrolidine-2-carboxamide (**27**). Following the general procedure and using L-prolinamide (42 mg, 0.4 mmol), compound **28** was obtained as a yellowish-white solid (82 mg, 74%) mp = 110 °C; ¹H NMR (DMSO-*d*₆) δ: 8.34 (d, *J* = 5.2 Hz, 1H), 7.86 (d, *J* = 7.6 Hz, 2H), 7.52 (d, *J* = 7.6 Hz, 2H), 7.30 (brs, 2H), 6.89 (d, *J* = 5.2 Hz, 1H), 4.42–4.40 (m, 1H), 3.67–3.50 (m, 2H), 2.71 (s, 3H), 2.22–2.18 (m, 1H), 1.95–1.90 (m, 3H), 1.29 (s, 9H); ¹³C NMR (DMSO-*d*₆) δ: 175.3, 166.6, 162.4, 159.7, 158.6, 154.5, 153.8, 131.2, 130.5, 126.0, 125.6, 106.9, 60.7, 46.8, 35.1, 31.2, 30.8, 23.9, 18.6; MS (*m/z*) 421; anal. calc. for: (C₂₃H₂₇N₅OS,



Mwt = 421): C, 65.53; H, 6.46; N, 16.61; found: C, 65.60; H, 6.51; N, 16.65%.

(*R*)-1-[4-[2-(4-(*tert*-Butyl)phenyl)-4-methylthiazol-5-yl]pyrimidin-2-yl]pyrrolidine-2-carboxamide (**28**). Following the general procedure and using *D*-prolinamide (42 mg, 0.4 mmol), compound **28** was obtained as a yellowish-white solid (100 mg, 90%) mp = 115 °C; ¹H NMR (DMSO-*d*₆) δ: 8.40 (d, *J* = 5.2 Hz, 1H), 7.88 (d, *J* = 7.6 Hz, 2H), 7.51 (d, *J* = 7.6 Hz, 2H), 7.38 (brs, 2H), 6.92 (d, *J* = 5.2 Hz, 1H), 4.46–4.43 (m, 1H), 3.60–3.56 (m, 2H), 2.68 (s, 3H), 2.20–2.19 (m, 1H), 1.95–1.90 (m, 3H), 1.29 (s, 9H); ¹³C NMR (DMSO-*d*₆) δ: 175.0, 166.6, 160.1, 159.0, 158.6, 154.0, 153.8, 131.9, 130.5, 126.5, 126.4, 106.8, 60.6, 47.6, 35.1, 31.3, 31.1, 23.6, 18.6; MS (*m/z*) 421; anal. calc. for: (C₂₃H₂₇N₅O₃, Mwt = 421): C, 65.53; H, 6.46; N, 16.61; found: C, 65.62; H, 6.53; N, 16.69%.

4.2. Microbiological assay

4.2.1 MIC determination and evaluation of antimicrobial activity. The MICs of test compounds and control drugs such as antibiotics (linezolid, vancomycin, gentamicin, cefixime) and antifungal drugs (amphotericin B and fluconazole) were determined using the broth-microdilution method according to guidelines outlined by the Clinical and Laboratory Standards Institute^{34,35} with some modifications against clinically relevant bacterial (MRSA, *E. coli*, *C. difficile*, and *N. gonorrhoea*) and fungal (*C. albicans*) strains. *S. aureus* and *E. coli* were grown aerobically overnight on tryptone soy agar plates at 37 °C. *C. difficile* was grown anaerobically on brain heart infusion-supplemented agar at 37 °C for 48 h. *N. gonorrhoea* was grown on *Brucella* broth supplemented with yeast extract, neopeptone, hematin, pyridoxal, and NAD at 37 °C for 24 h in an atmosphere of 5% CO₂. *C. albicans* was grown aerobically overnight on yeast peptone dextrose agar plates at 35 °C. Afterwards, a bacterial solution equivalent to 0.5 McFarland standard was prepared and diluted in cation-adjusted Mueller–Hinton broth (for *S. aureus* and *E. coli*) to achieve a concentration of $\sim 5 \times 10^5$ CFU mL⁻¹. *C. difficile* was diluted in brain heart infusion-supplemented broth supplemented with yeast extract, hemin, and vitamin K to achieve a concentration of $\sim 5 \times 10^5$ CFU mL⁻¹. *N. gonorrhoeae* was diluted in *Brucella* broth supplemented with yeast extract, neopeptone, hematin, pyridoxal and NAD to achieve a concentration of $\sim 1 \times 10^6$ CFU mL⁻¹. *C. albicans* was diluted in Roswell Park Memorial Institute 1640 medium with glutamine and without bicarbonate, which was buffered to pH 7.0 with 0.165 M of [3-(*N*-morpholino)propanesulfonic acid] to achieve a concentration of $\sim 1.5 \times 10^3$ CFU mL⁻¹. Compounds and control drugs were added in the first row of 34-well plates and serially diluted with the corresponding media containing bacteria/fungi. Then, plates were incubated as described previously. The MICs reported in Table 1 denote the minimum concentration of compounds and control drugs that could completely inhibit the visual growth of bacteria/fungi.

4.3. Studies on metabolism simulation

To validate the metabolic resistance and bioavailability of new compound **20** compared with lead compounds **1a** and **1c**,

certain molecular parameters were calculated, and metabolism simulation was performed. First, calculations using SWISS-ADME, MolSoft, and Discovery Studio 4.1 were conducted for data comparison and validation from discrete sources. Compound **19** was similar in all properties to compound **20** because they were structural isomers, so compound **20** was designated for studies. The structures of compounds were drawn using ChemDraw v.2014 and saved in a readable mol extension. Online free platforms such as SWISSADME and MolSoft were selected to ascertain expected molecular properties and expected interaction with prominent metabolic enzymes *via* structural upload and RUN. Validation through calculations of ADME descriptors using Discovery Studio after compound preparation and application of CHARMM forcefield was done. Metabolism simulation was developed using PK-Sim software after data insertion of pK_a, molecular properties, and assuming drug-dose administration as a single intravenous infusion.

Conflicts of interest

There are no conflicts to declare.

Acknowledgements

This paper is based on work supported by Science, Technology and Innovation Funding Authority under grant number 43229 for young researchers.

References

- 1 D. Schillaci, V. Spanò, B. Parrino, A. Carbone, A. Montalbano, P. Barraja, P. Diana, G. Cirrincione and S. Cascioferro, *J. Med. Chem.*, 2017, **60**, 8268–8297.
- 2 B. Parrino, D. Carbone, G. Cirrincione, P. Diana and S. Cascioferro, *Futur. Med. Chem.*, 2019, **12**, 326.
- 3 B. Aslam, W. Wang, M. I. Arshad, M. Khurshid, S. Muzammil, M. H. Rasool, M. A. Nisar, R. F. Alvi, M. A. Aslam and M. U. Qamar, *Infect. Drug Resist.*, 2018, **11**, 1645.
- 4 S. S. Kadri, *Crit. Care Med.*, 2020, 7176261.
- 5 A. Hassoun, P. K. Linden and B. Friedman, *Crit. Care*, 2017, **21**, 211.
- 6 A. S. Lee, H. de Lencastre, J. Garau, J. Kluytmans, S. Malhotra-Kumar, A. Peschel and S. Harbarth, *Nat. Rev. Dis. Primers*, 2018, **4**, 1–23.
- 7 R. M. Hassan, M. G. Elanany, M. M. Mostafa, R. H. A. Yousef and S. T. Salem, *J. Microbiol., Immunol. Infect.*, 2023, **56**(4), 802–814.
- 8 J. Fishovitz, J. A. Hermoso, M. Chang and S. Mobashery, *IUBMB Life*, 2014, **66**, 572–577.
- 9 P. Wiegand, D. Nathwani, M. Wilcox, J. Stephens, A. Shelbaya and S. Haider, *J. Hosp. Infect.*, 2012, **81**, 1–14.
- 10 P. A. Myer, A. Mannalithara, G. Singh, G. Singh, P. J. Pasricha and U. Ladabaum, *Am. J. Gastroenterol.*, 2013, **108**, 1496–1507.



- 11 L. C. McDonald, M. Owings and D. B. Jernigan, *Emerg. Infect. Dis.*, 2006, **12**, 3291455.
- 12 M. L. Manning, J. Pfeiffer and E. L. Larson, *Am. J. Infect. Control*, 2016, **44**, 1454–1457.
- 13 H. Grundmann, M. Aires-de-Sousa, J. Boyce and E. Tiemersma, *Lancet*, 2006, **368**, 874–885.
- 14 L. Ravindar, S. Bukhari, K. Rakesh, H. Manukumar, H. Vivek, N. Mallesha, Z.-Z. Xie and H.-L. Qin, *Bioorg. Chem.*, 2018, **81**, 107–118.
- 15 H. F. Chambers, *N. Engl. J. Med.*, 2005, **352**, 1485–1487.
- 16 G. J. Moran, A. Krishnadasan, R. J. Gorwitz, G. E. Fosheim, L. K. McDougal, R. B. Carey and D. A. Talan, *N. Engl. J. Med.*, 2006, **355**, 666–674.
- 17 B. W. Frazee, J. Lynn, E. D. Charlebois, L. Lambert, D. Lowery and F. Perdreau-Remington, *Ann. Emerg. Med.*, 2005, **45**, 311–320.
- 18 S. K. Fridkin, J. C. Hageman, M. Morrison, L. T. Sanza, K. Como-Sabetti, J. A. Jernigan, K. Harriman, L. H. Harrison, R. Lynfield and M. M. Farley, *N. Engl. J. Med.*, 2005, **352**, 1436–1444.
- 19 G. J. Moran, R. N. Amii, F. M. Abrahamian and D. A. Talan, *Emerging Infect. Dis.*, 2005, **11**, 928.
- 20 K. Hiramatsu, *Lancet Infect. Dis.*, 2001, **1**, 147–155.
- 21 P. Wilson, J. Andrews, R. Charlesworth, R. Walesby, M. Singer, D. Farrell and M. Robbins, *J. Antimicrob. Chemother.*, 2003, **51**, 186–188.
- 22 S. Lin, J.-J. Koh, T. T. Aung, F. Lim, J. Li, H. Zou, L. Wang, R. Lakshminarayanan, C. Verma and Y. Wang, *J. Med. Chem.*, 2017, **60**, 1362–1378.
- 23 H. Mohammad, A. S. Mayhoub, A. Ghafoor, M. Soofi, R. A. Alajlouni, M. Cushman and M. N. Seleem, *J. Med. Chem.*, 2014, **57**, 1609–1615.
- 24 I. Eid, M. M. Elsebaei, H. Mohammad, M. Hagra, C. E. Peters, Y. A. Hegazy, B. Cooper, J. Pogliano, K. Pogliano and H. S. Abulkhair, *Eur. J. Med. Chem.*, 2017, **139**, 665–673.
- 25 E. Yahia, H. Mohammad, T. M. Abdelghany, E. Fayed, M. N. Seleem and A. S. Mayhoub, *Eur. J. Med. Chem.*, 2017, **126**, 604–613.
- 26 M. A. Seleem, A. M. Disouky, H. Mohammad, T. M. Abdelghany, A. S. Mancy, S. A. Bayoumi, A. Elshafeey, A. El-Morsy, M. N. Seleem and A. S. Mayhoub, *J. Med. Chem.*, 2016, **59**, 4900–4912.
- 27 Y. Cheng, F. Zhang, T. A. Rano, Z. Lu, W. A. Schleif, L. Gabryelski, D. B. Olsen, M. Stahlhut, C. A. Rutkowski and J. H. Lin, *Bioorg. Med. Chem. Lett.*, 2002, **12**, 2419–2422.
- 28 A. Kotb, N. S. Abutaleb, M. A. Seleem, M. Hagra, H. Mohammad, A. Bayoumi, A. Ghiaty, M. N. Seleem and A. S. Mayhoub, *Eur. J. Med. Chem.*, 2018, **151**, 110–120.
- 29 Clinical and Laboratory Standards Institute, *M7-A9*, Wayne, PA, 9th edn, 2012.
- 30 Clinical and Laboratory Standards Institute, *M29*, Wayne, PA, 2007.
- 31 Clinical and Laboratory Standards Institute, *Approved Standard M27-A3*, Wayne, PA, 3rd edn, 2008.
- 32 S. B. Olasupo, A. Uzairu, G. A. Shallangwa and S. Uba, *Future J. Pharm. Sci.*, 2021, **7**, 1–10.
- 33 D. Teutonico, M. Block, L. Kuepfer, J. Solodenko, T. Eissing and K. Coboeken, *Oral Drug Delivery for Modified Release Formulations*, 2022, pp. 375–389.
- 34 P. Wayne, *CLSI Document M27-A2*, 2002.
- 35 T. A. Geers and A. M. Donabedian, *Antimicrob. Agents Chemother.*, 1989, **33**, 233–234.

